Nonautonomous deformed solitons in a Bose–Einstein condensate*

Li Ze-Jun(李泽军), Hai Wen-Hua(海文华)†, and Deng Yan(邓 艳)

Department of Physics and Key Laboratory of Low-Dimensional Quantum Structure and Quantum Control of Ministry of Education, Hunan Normal University, Changsha 410081, *China*

(Received 21 January 2013; revised manuscript received 8 April 2013)

We study exact single-soliton solutions of an attractive Bose–Einstein condensate governed by a one-dimensional nonautonomous Gross–Pitaevskii system. For several different forms of time-dependent atom–atom interaction and external parabolic potential which satisfy the exact integrability scenario, we construct a set of new analytical nonautonomous deformed-soliton solutions, including the macroscopic wave function and the position of soliton's center of mass. The soliton characteristics are modulated by the external field parameters and deformation factors related to the number of the condensed atoms and the initial conditions. The results suggest a simple and effective method for experimentally generating matter-wave deformed solitons and manipulating their motions.

Keywords: Bose–Einstein condensate, nonautonomous system, deformed soliton

PACS: 05.45.Yv, 03.75.Kk, 03.65.Ge, 03.75.Lm **DOI:** 10.1088/1674-1056/22/9/090505

1. Introduction

Matter-wave solitons in a Bose–Einstein condensate (BEC) have historically attracted a lot of attention due to its possible relevance to many areas of physics. Recently, people have created bright, dark, and gap matter-wave solitons in BEC by using various methods.[1–10] Such soliton motions are governed by the Gross–Pitaevskii equation (GPE) with different external potentials, which have been investigated theoretically and experimentally.[11–15] When the external potential is time-dependent, the GPE becomes a nonautonomous nonlinear Schrödinger equation (NLSE).[16–18] Generally, it is very difficult to obtain the exact analytical solution of the nonautonomous NLSE, because of its nonintegrability. By using the effective-particle approximation,[16,17] the soliton states in terms of its position and velocity have been investigated for such systems, and it has been found that the average velocity of a soliton depends on the number of condensed atoms in the soliton.

An analytically exact solution, of course, can provide deeper understanding of the underlying physics than straight numerical calculations. Therefore, several different methods were adopted to analytically solve the autonomous and nonautonomous NLSE.[19–25] One of the famous methods is the Darboux transformation which can be used to construct the exact solutions of the NLSE under some particular conditions.[19–22] Lately, Serkin *et al.* studied the generalized nonautonomous NLSE with time-dependent dispersion, nonlinearity, and gain or loss, and established the scenario to judge whether the system is integrable.[26] Based on the exact integrability scenario, they obtained the relationship between the atom–atom interactions and the external parabolic potentials, and offered the exact nonautonomous soliton solutions of the NLSE.[26–28] Such exact solutions have greater significance for testing the validity of the GPE at high densities and for investigating the time evolution of the nonautonomous solitons.[19]

It is well known that a lot of exact one-soliton solutions have been reported for different physical systems,[29–35] where the soliton amplitudes were consistently described by a standard hyperbolic secant function of spatiotemporal coordinates. In Ref. [36], we considered a class of deformed-soliton solutions, and studied its ratchet effect. In this paper, for several different forms of the time-dependent atom–atom interaction and external parabolic potential which satisfy the exact integrability scenario, we gain different new nonautonomous deformed-soliton solutions. They describe some new soliton characteristics of the attractive BEC. We define the deformation factor modulated by the number of condensed atoms and the initial conditions, and mathematically demonstrate that one can change the position of the matter-wave soliton and its propagation velocity by adjusting the deformation factor. The results can be generalized to other physical systems governed by the NLSE.

This paper is organized as follows. We demonstrate the exact nonautonomous deformed-soliton solutions in Section 2. In Section 3, we study the dynamical behaviors of the deformed solitons for different physical cases. Finally, we summarize our results in Section 4.

2. Exact nonautonomous deformed-soliton solutions

We consider a one-dimensional BEC system in a time-dependent parabolic potential. The governing dimensionless

*Project supported by the National Natural Science Foundation of China (Grant No. 11175064).

†Corresponding author. E-mail: whhai2005@yahoo.com.cn

© 2013 Chinese Physical Society and IOP Publishing Ltd

GPE reads[27]

$$\mathrm{i}\frac{\partial Q(x,t)}{\partial t}+\frac{1}{2}\frac{\partial^2 Q(x,t)}{\partial x^2}+R(t)|Q(x,t)|^2Q(x,t)-\frac{1}{2}\Omega^2(t)x^2Q(x,t)=0, \quad (1)$$

where $\Omega^2(t)$ and $R(t)$ denote the time-dependent strengths of the parabolic potential and the atom–atom interaction, respectively. The positive sign of $\Omega^2(t)$ is related to the harmonic potential and the negative sign is related to the inverted harmonic potential.[27] Similarly, the positive $R(t)$ is associated with the attractive interaction and the negative $R(t)$ is associated with the repulsive interaction. In this paper, we study the bright-soliton solution of Eq. (1) for the attractive interaction with $R(t)>0$. For simplification, hereafter we adopt dimensionless parameters in standard soliton units, as they are commonly known.[26,27,36]

Applying the exact integrability scenario[26] to Eq. (1) and setting $R(t)=R_0/\Phi(t)$, we know that the system is exactly solvable if the relation

$$\ddot{\Phi}+\Omega^2\Phi=0, \quad \Phi=R_0/R, \quad (2)$$

is satisfied between the time-varying nonlinearity and external potential, with constant R_0 being the initial interaction strength. For a given parabolic potential strength, the atom–atom interaction is determined by Eq. (2). If both the strength of parabolic potential and the atom–atom interaction are determined by Eq. (2), the form of function $\Phi(t)$ is determined entirely. In this paper, we will consider the cases in which the strengths of the parabolic potential and atom–atom interactions are known, as did in Ref. [27], and treat $\Phi(t)$ as the corresponding known functions.

In previous work,[31,37,38] we have used the method of ansatz solution to analytically study the GPEs. Here we take the exact deformed-soliton solution[36] into Eq. (1) in the form of

$$\begin{aligned} Q(x,t) &= r(x,t)\,\mathrm{e}^{\mathrm{i}S(x,t)},\\ r(x,t) &= \frac{h(t)}{\mathrm{e}^{d(t)x+f(t)}+k\,\mathrm{e}^{-d(t)x-f(t)}},\\ S(x,t) &= A(t)x^2+B(t)x+C(t), \end{aligned} \quad (3)$$

where $A(t)$, $B(t)$, $C(t)$, $d(t)$, $h(t)$, and $f(t)$ are the undetermined functions, k is the deformed factor determined by the initial conditions and physical parameters, and $r(x,t)$ and $S(x,t)$ denote the amplitude and phase of the soliton, respectively. Clearly, Eq. (3) denotes a kind of new single soliton solutions. Differing from the standard one-soliton solution of the hyperbolic secant form given in Refs. [26] and [27], the deformed factor $k\neq 1$ enables the one-soliton solution to deviate from the standard shape. For different nonlinearity and corresponding external parabolic potential, we can obtain different deformed-soliton solutions, and then study the influence of the deformation factor k on the deformed soliton motions in different external potentials.

Inserting Eq. (3) into Eq. (1), we derive the coupled equations of the undetermined functions as

$$\dot{A}+2A^2+\frac{1}{2}\Omega^2=0, \quad \dot{B}+2AB=0,$$
$$\dot{d}+2Ad=0, \quad \dot{h}+Ah=0, \quad \dot{f}+Bd=0, \quad (4)$$
$$\dot{C}+\frac{1}{2}B^2-\frac{1}{2}d^2=0, \quad d^2-\frac{Rh^2}{4k}=0. \quad (5)$$

The first expression in Eq. (4) is just the Riccati equation on the undetermined function $A(t)$, which can be solved exactly. Given the exact solution $A(t)$ as an explicit function of time, the other equations of Eqs. (4) and (5) can be decoupled and be solved for other undetermined functions. It is well known that the solution of the Riccati equation can be expressed by the solution of the harmonic-oscillator equation (3).[37,39] Setting $A(t)=\dot{\Phi}/(2\Phi)$ and using $\Phi(t)$ as a known function, from Eqs. (4) and (5) we obtain the undetermined functions and the deformation factor k as

$$A(t)=\frac{\dot{\Phi}}{2\Phi}, \quad B(t)=\frac{B_0}{\Phi}, \quad C(t)=\frac{1}{2}\int\frac{d_0^2-B_0^2}{\Phi^2}\,\mathrm{d}t,$$
$$d(t)=\frac{d_0}{\Phi}, \quad h(t)=\sqrt{\frac{h_0}{\Phi}}, \quad f(t)=-\int\frac{B_0d_0}{\Phi^2}\,\mathrm{d}t, \quad k=\frac{h_0R_0}{4d_0^2}. \quad (6)$$

Here, B_0, d_0, and h_0 are the integration constants determined by the initial conditions. Clearly, the functions $B(t)$, $d(t)$, and $h^2(t)$ have the same function forms with only some different constant factors. A similar relation exists between the functions $C(t)$ and $f(t)$. From Eqs. (3) and (6), we know that B_0 is related to the initial phase, d_0 and h_0 are associated with the initial width and height of the soliton. The constant k is adjusted by the integration constants and the initial interaction strength $R_0=4\pi\hbar^2a_{\mathrm{s}}(0)/m$, where $a_{\mathrm{s}}(0)$ is the s-wave scattering length at $t=0$. From Eq. (6), we can see that once the function $\Phi(t)=R_0/R$ is given, all the undetermined functions in Eq. (3) will have explicit forms, then Eq. (3) becomes the exact deformed-soliton solution. Substituting Eqs. (3) and (6) into the normalization condition $\int_{\infty}^{\infty}|\psi(x,t)|^2\,\mathrm{d}x=N$ yields

$$k=\frac{h_0}{2d_0N}, \quad (7)$$

with N being the number of condensed atoms. Equation (7) implies that we can adjust the deformed factor by changing the number of condensed atoms. Combining the last formula in Eq. (6) with Eq. (7), we gain the relationship between the atomic number N and the initial constants as

$$N=\frac{2d_0}{R_0}. \quad (8)$$

This relationship implies that for an experimentally given atomic number N, to produce the deformed-soliton solution (3), the initial conditions must be confined by Eq. (8).

It is mathematically well-known that any special solution of Eq. (1) is associated with a set of special initial and boundary conditions. Particularly, for the bright-soliton case as well as zero boundary conditions, different special solutions are determined only by different initial conditions. For the deformed-soliton solution (3), the deformation factor k is related to the number of condensed atoms according to Eq. (7).

Much work is focused on the position and velocity, with the soliton acting as a quasi-particle.[16,17,40] Given the exact deformed-soliton solutions, we can easily establish the exact formulas of the position and velocity. Applying the extremum theorem to Eq. (3), from $[\partial|Q(x,t)|^2/\partial x]_{x=x_c}=0$ we derive the position formula of the atomic density peak as

$$x_c=\frac{1}{2d}(\ln k-2f). \tag{9}$$

The corresponding velocity formula is $v_c=\dot{x}_c$. For a standard one-soliton solution with $k=1$ and $\ln k=0$, equation (9) is reduced to the well-known position of the soliton's center of mass. In the presence of a perturbation, it has been studied by using the effective-particle approximation.[16,17] Obviously, the position and velocity of the deformed soliton with $k\neq 1$ and $\ln k\neq 0$ completely differ from those of the standard soliton. Substituting $d(t)$, $f(t)$, and k given by Eq. (6) into Eq. (9), we here can exactly show the position and velocity of the soliton's center of mass, and study the influence of the deformation factor k on the soliton motions.

3. Dynamical behaviors of the deformed solitons

For different nonlinearity, by means of Eq. (2), the external parabolic potential is only confirmed. In Ref. [27], the authors have given several different function forms of the nonlinearity strength $R(t)$ and parabolic potential strength $\Omega^2(t)$. Using different function pairs of $R(t)$ and $\Omega(t)$ which satisfy the exact integrability scenario, we construct several different deformed one-soliton solutions. Here we will investigate the dynamical behaviors of different deformed solitons.

3.1. Spatiotemporal evolutions of the deformed solitons near the Feshbach resonance

When the magnetic field is near the Feshbach resonance, the s-wave scattering length $a_s(t)$ can be tuned linearly or exponentially.[22,27,41] Corresponding to the nonlinearity $R(t)$, the time-dependent frequency function $\Omega(t)$ is also confirmed only by means of the exact integrability scenario. We will study the dynamics behavior of the deformed soliton under different cases.

Case 1 Linearly variable nonlinearity Inserting such a nonlinearity into Eq. (2) produces the function pair of $R(t)$ and $\Omega(t)$ as[27]

$$R(t)=1+\gamma_1 t,\quad \Omega^2(t)=-\frac{2\gamma_1^2}{(1+\gamma_1 t)^2}, \tag{10}$$

where γ_1 is a constant adjusted by the magnetic field. Using Eq. (2) and the last formula in Eq. (6), we obtain the function $\Phi(t)=R_0/R(t)=4kd_0^2/[h_0(1+\gamma_1 t)]$. Utilizing the function $\Phi(t)$ and Eq. (6), we arrive at the concrete forms of the undetermined functions as follows:

$$\begin{aligned}
A(t) &= -\frac{\gamma_1}{2(1+\gamma_1 t)},\quad B(t)=\frac{B_0h_0(1+\gamma_1 t)}{4kd_0^2},\\
C(t) &= \frac{h_0^2}{32k^2d_0^2}\left(1-\frac{B_0^2}{d_0^2}\right)\left(t+\gamma_1 t^2+\frac{1}{3}\gamma_1^2t^3\right)+C_0,\\
d(t) &= \frac{h_0(1+\gamma_1 t)}{4kd_0},\quad h(t)=\sqrt{\frac{h_1^2(1+\gamma_1 t)}{4kd_0^2}},\\
f(t) &= -\frac{B_0h_0^2}{16k^2d_0^3}\left(t+\gamma_1 t^2+\frac{1}{3}\gamma_1^2t^3\right)+f_0.
\end{aligned} \tag{11}$$

Inserting Eq. (11) into Eq. (3), we obtain the explicit form of the deformed-soliton solution.

By combining Eq. (3) with Eq. (11), the spatiotemporal evolution of the deformed soliton with $k=0.8$ is shown in Fig. 1. The other parameters are taken as $\gamma_1=1$, $B_0=1$, $d_0=2$, $h_0=1$, and $f_0=1$. For fixed d_0 and h_0, equations (7) and (8) mean that different k values correspond to different atomic numbers N and initial interactions R_0. From Fig. 1, we find the self-compression behavior of the nonautonomous deformed soliton. With the increase in time, the solitonic width is compressed continuously so that the solitonic height increases simultaneously. Physical reason for the self-compression is the linear increase of the nonlinearity strength.

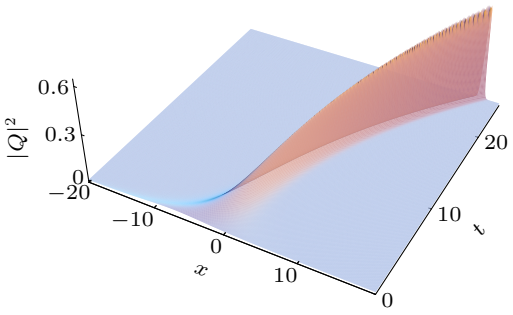


Fig. 1. (color online) Spatiotemporal evolution of the atomic density $|Q(x,t)|^2$ for the deformed soliton with $k=0.8$. Other parameters are $\gamma_1=1$, $B_0=1$, $d_0=2$, $h_0=1$, and $f_0=1$.

By means of Eq. (9), the trajectories of atomic density peaks are illustrated in Fig. 2 for the standard soliton with $k=1$ and the deformed solitons with $k=0.5$ and $k=2$, respectively. Comparing the three curves in Fig. 2, we can see that the motion velocities of density peaks, $v_c=\dot{x}_c$, are different for different deformation factors. The dashed curve shows that at $t\approx 4$ the standard soliton varies its velocity from negative to positive, then the corresponding position x_c increases monotonically. The thick solid curve indicates the monotone increasing position of the deformed soliton with the smaller value $k=0.5$. The thin solid lines indicate that for the deformation factor $k=2$, the soliton position decreases from $t=0$

to $t \approx 10$, and then increases monotonically. Clearly, before $t \approx 10$, the solitons may change their motion directions. However, after $t \approx 10$, the three different solitons propagate toward right with different speeds, and the speed increases with the decrease in the deformation factor. Thus, the motion velocity of the soliton can be adjusted by changing the deformation factor k, or equivalently, changing the number of condensed atoms and the initial conditions. Such a change of the factor k will lead to deformation of the soliton.[36] Therefore, we can modulate the motion velocity of the deformed soliton simultaneously.

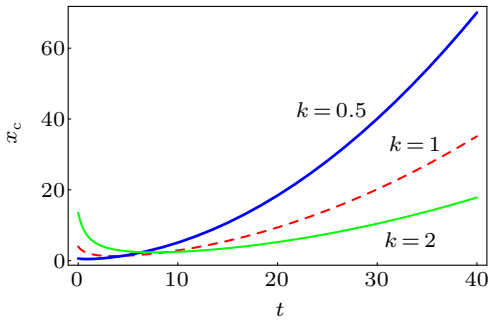


Fig. 2. (color online) The trajectories of atomic density peaks for $k = 1$ (dashed curve), $k = 0.5$ (thick solid curve), and $k = 2$ (thin solid curve). The other parameters are the same as those in Fig. 1.

Case 2 Exponentially variable nonlinearity In such a case, the function pair of $R(t)$ and $\Omega(t)$ reads[27]

$$R(t) = \mathrm{sech}(\gamma_2 t), \quad \Omega^2(t) = -\gamma_2^2, \tag{12}$$

where γ_2 is a constant adjusted by the magnetic field. The negative constant Ω^2 implies that the external potential is a inverted harmonic one. A detailed study has been carried out in Refs. [22] and [31] for this case. Hence, here we mainly research the influence of factor k on the movement of soliton. Inserting R_0 in Eq. (6) into Eq. (2), we obtain $\Phi(t) = R_0/R = 4kd_0^2/[h_0 \mathrm{sech}(\gamma_2 t)]$. The undetermined functions can be derived from Eq. (6) as

$$\begin{aligned}
A(t) &= \gamma_2 \tanh(\gamma_2 t), \quad B(t) = \frac{B_0 h_0}{4kd_0^2}\mathrm{sech}(\gamma_2 t), \\
C(t) &= \frac{(d_0^2 - B_0^2)h_0^2}{64k^2 d_0^4 \gamma_2}\tanh(\gamma_2 t) + C_0, \\
d(t) &= \frac{h_0}{4kd_0}\mathrm{sech}(\gamma_2 t), \quad h(t) = \frac{h_0}{2d_0\sqrt{k}}\sqrt{\mathrm{sech}(\gamma_2 t)}, \\
f(t) &= -\frac{d_0 B_0 h_0^2}{16k^2 d_0^4 \gamma_2}\tanh(\gamma_2 t) + f_0.
\end{aligned} \tag{13}$$

According to Eqs. (13) and (3), we obtain the deformed-soliton solution. Combining Eq. (13) with Eq. (9), we obtain the trajectory of atomic density peak, which is plotted in Fig. 3 with $d_0 = 1$, $\gamma_2 = 1$, $B_0 = 1$, $h_0 = 1$, $f_0 = 1$, and different deformation factors, i.e., $k = 1$, $k = 0.12$, and $k = 6$.

Figure 3 shows that for the deformation factors $k \geq 1$, the two solitons propagate with the same direction and different speeds. The speed of the deformed soliton with $k = 6$ is slower than that of the standard soliton. The propagation direction of the soliton is reversed and its speed is increased, when the k value is changed to $k = 0.12$. Therefore, the motion direction of the soliton can be adjusted by changing the deformation factor k. The change in the factor k will cause change in the soliton shape.[36] Similar to Case 1, we can modulate the shape and motion velocity of the deformed soliton simultaneously. However, here the average velocities of solitons, $\bar{x}_c(\tau) = (1/\tau)\int_0^\tau \dot{x}_c \mathrm{d}t$ for a larger time τ, are much greater than that for Case 1, because of the difference between the exponentially and linearly variable nonlinearities.

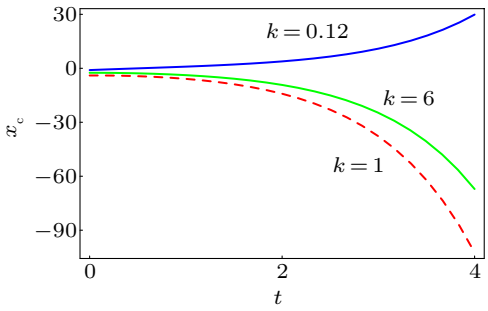


Fig. 3. (color online) The trajectories of atomic density peaks for $d_0 = 1$, $\gamma_2 = 1$, $B_0 = 1$, $h_0 = 1$, and $f_0 = 1$. The deformation factor is taken as $k = 1$ (dashed curve), $k = 0.12$ (thick solid curve), and $k = 6$ (thin solid curve).

3.2. Spatiotemporal evolutions of the deformed solitons with periodically variable nonlinearity

It is well known that for a periodic magnetic field the s-wave scattering length can be a periodic function, whose frequency is the same as that of the magnetic field. Such periodic nonlinearity includes two cases, namely, it can be proportional to or inversely proportional to a sinusoidal function.[27]

Case 3 Nonlinearity proportional to a sinusoidal function Applying such a nonlinearity to Eq. (2) yields[27]

$$\begin{aligned}
R(t) &= 1 + \gamma_3 \sin(\omega_1 t), \\
\Omega^2(t) &= -\frac{\gamma_3 \omega_1^2 [\gamma_3 + \gamma_3 \cos^2(\omega_1 t) + \sin(\omega_1 t)]}{[1 + \gamma_3 \sin(\omega_1 t)]^2},
\end{aligned} \tag{14}$$

with γ_3 being a constant adjusted by the magnetic field. It can be seen from Eq. (14) that for constant $|\gamma_3| > 1$, the parabolic potential keeps an inverted harmonic one. When $|\gamma_3| < 1$ is set, the parabolic potential periodically varies its sign between harmonic and inverted harmonic potentials. The periodic variation features of nonautonomous soliton in a periodically driven parabolic potential are studied in Refs. [27], [42], and [43], where the period of time evolution of the standard soliton is the period of the external potential ($2\pi/\omega_1$). In this section, we mainly study some properties of the deformed soliton. Using Eqs. (2) and (6), we have $\Phi(t) = 4kd_0^2/(h_0 R)$. Combining

this expression with Eqs. (6) and (14), the undetermined functions in Eq. (3) are expressed as

$$A(t) = -\frac{\omega_1\gamma_3\cos(\omega_1 t)}{2[1+\gamma_3\sin(\omega_1 t)]},\quad B(t) = \frac{B_0 h_0[1+\gamma_3\sin(\omega_1 t)]}{4kd_0^2},$$
$$C(t) = -\frac{(d_0^2-B_0^2)h_0^2}{32\omega_1 k^2 d_0^2}\Big[\omega_1 t + \frac{\omega_1 t\gamma_3^2}{2} - 2\gamma_3\cos(\omega_1 t) - \frac{1}{4}\gamma_3^2\sin(2\omega_1 t)\Big] + C_0,$$
$$d(t) = \frac{h_0}{4kd_0}[1+\gamma_3\sin(\omega_1 t)],\quad h(t) = \sqrt{\frac{h_0^2}{4kd_0^2}[1+\gamma_3\sin(\omega_1 t)]},$$
$$f(t) = \frac{B_0 d_0 (h_0)^2}{16\omega_1 k^2 d_0^2}\Big[\omega_1 t + \frac{\omega_1\gamma_3^2 t}{2} - 2\gamma_3\cos(\omega_1 t) - \frac{1}{4}\gamma_3^2\sin(2\omega_1 t)\Big] + f_0. \quad (15)$$

From Eq. (15), for $\gamma_3 = 0.5$ and $\omega_1 = 0.8$, time evolutions of the nonlinearity and the parabolic potential $V(t) = x_0^2\Omega^2(t)/2$ with $x_0 = 2$ are plotted in Fig. 4(a), respectively. The spatiotemporal evolution of soliton density for $k = 0.8$ is shown in Fig. 4(b).

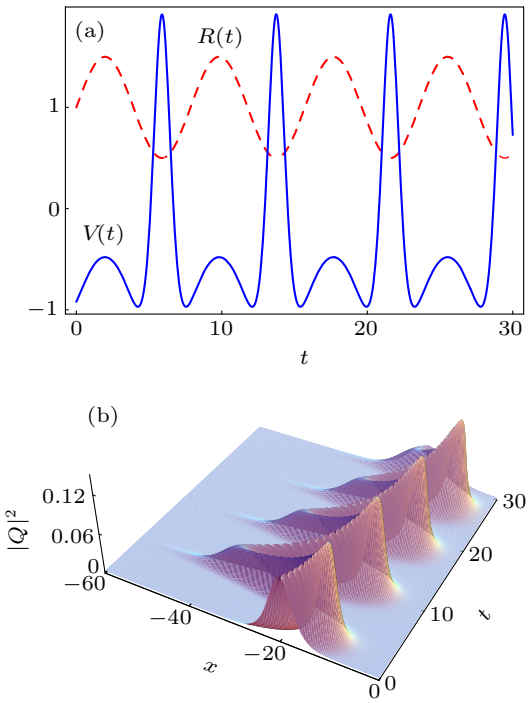


Fig. 4. (color online) (a) Time evolutions of the nonlinearity (dashed line) and parabolic potential (solid line) for $\omega_1 = 0.8$, $\gamma_3 = 0.5$, and $x = x_0 = 2$. (b) Spatiotemporal evolution of the soliton density for $B_0 = 1$, $h_0 = 1$, $f_0 = 6$, $d_0 = 1$, and $k = 0.8$.

It is noted from Fig. 4(a) that the external potential can change not only its amplitude but also its sign that means the transformation between the harmonic trap and inverted harmonic barrier. The positive $R(t)$ confirms the attractive interaction. From Fig. 4(b), we see that the amplitude and width of the deformed soliton oscillates periodically, due to the modulation of the external periodic field. When the soliton amplitude increases (or decreases), the soliton width becomes narrow (or wide).

Now, we consider the effect of the deformation factor k on the soliton motion. Setting $\gamma_3 = 0.8$, $B_0 = 1$, $d_0 = 1$, $h_0 = 1$, $f_0 = 1$, and $\omega_1 = 2$, combining Eq. (15) with Eq. (9), we plot the trajectory of the soliton density peak for $k = 1$ and $k = 0.2$ respectively in Figs. 5(a) and 5(b). It is worth noting that function $f(t)$ in Eq. (15) contains the terms proportional to time t and periodic functions, and the second term of Eq. (9) is proportional to $f(t)$. Therefore, the trajectory x_c of the soliton oscillates aperiodically.

It can be seen from Fig. 5 that for different deformation factors k, the trajectory, velocity, and the oscillation range of the solitons are different. As shown in Fig. 5(a), we see that for $t < 10$ the standard soliton oscillates aperiodically in the range of $x_c < 0$. With the increase in time, it oscillates in the range of $x_c > 0$ and the oscillation amplitude is less than 10 for the time interval of $0 \le t < 20$. However, figure 5(b) shows that the deformed soliton with $k = 0.2$ oscillates with a very large amplitude in the range of $x_c > 0$. From both figures, we know that for both cases the soliton always oscillates aperiodically and the oscillation amplitude increases with time. The high-speed oscillation of soliton will lead to loss of the system stability.

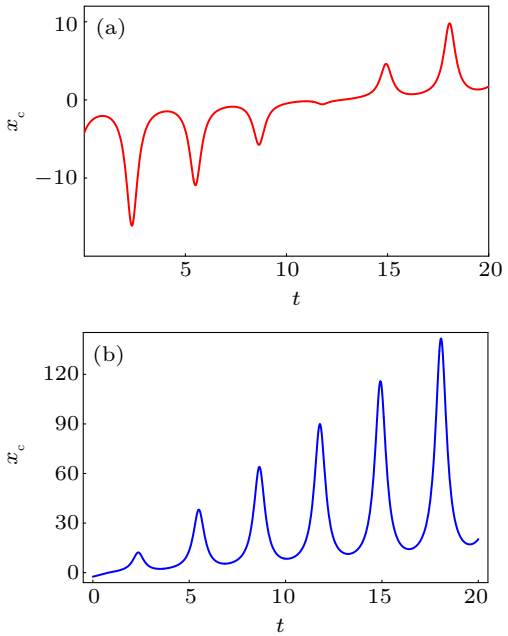


Fig. 5. (color online) The trajectory of soliton density peak for $\omega_1 = 2$, $\gamma_3 = 0.8$, $B_0 = 1$, $h_0 = 1$, $f_0 = 1$, and $d_0 = 1$. (a) $k = 1$; (b) $k = 0.2$.

Case 4 Nonlinearity inversely proportional to a sinusoidal function Such a case implies the function pair[27]

$$R(t) = \frac{1}{1+\gamma_4\sin(\omega_2 t)},\quad \Omega^2(t) = \frac{\gamma_4\omega_2^2\sin(\omega_2 t)}{1+\gamma_4\sin(\omega_2 t)}. \quad (16)$$

Here, γ_4 is a constant adjusted by the magnetic field. The periodic $\Omega^2(t)$ means that the parabolic potential transforms periodically between harmonic and inverted harmonic ones. Using Eqs. (2) and (6), we obtain $\Phi = 4kd_0^2/(h_0 R)$. Substituting it and Eq. (16) into Eq. (6), we have

$$A(t) = \frac{\omega_2\gamma_4\cos(\omega_2 t)}{2[1+\gamma_4\sin(\omega_2 t)]}, \quad B(t) = \frac{B_0 h_0}{4kd_0^2[1+\gamma_4\sin(\omega_2 t)]},$$
$$C(t) = \frac{(d_0^2-B_0^2)h_0^2}{32\omega_2 k^2 d_0^4}\left[\frac{-\gamma_4\sqrt{1-\gamma_4^2}\cos(\omega_2 t)-2\arctan\left[(\gamma_4+\tan(\omega_2 t)/2)/\sqrt{1-\gamma_4^2}\right][1+\gamma_4\sin(\omega_2 t)]}{\sqrt[3/2]{1-\gamma_4^2}[1+\gamma_4\sin(\omega_2 t)]}\right]+C_0,$$
$$d(t) = \frac{h_0}{4kd_0[1+\gamma_4\sin(\omega_2 t)]}, \quad h(t) = \sqrt{\frac{h_0^2}{4kd_0^2[1+\gamma_4\sin(\omega_2 t)]}}, \quad f(t) = -\frac{2B_0 d_0}{(d_0^2-B_0^2)}[C(t)-C_0]+f_0. \tag{17}$$

Applying functions $d(t)$ and $f(t)$ to Eq. (9) results in the position $x_c(t)$ of density peak, which is a complicated function.

Let $\gamma_4 = 0.6$, $\omega_2 = 1.4$, and the other parameters be the same as those in Fig. 5, we show the spatiotemporal evolutions of one-soliton densities for $k = 1$ and $k = 0.4$, respectively, as shown in Figs. 6(a) and 6(b).

From Fig. 6, we observe that the shape of the deformed soliton with $k = 0.4$ is changed compared to the standard soliton, the height of the deformed soliton is increased, the soliton width is compressed, and the wavepacks shift toward the right. Thus, the position, speed, and amplitude of the density peaks can be modulated by changing the deformation factor k.

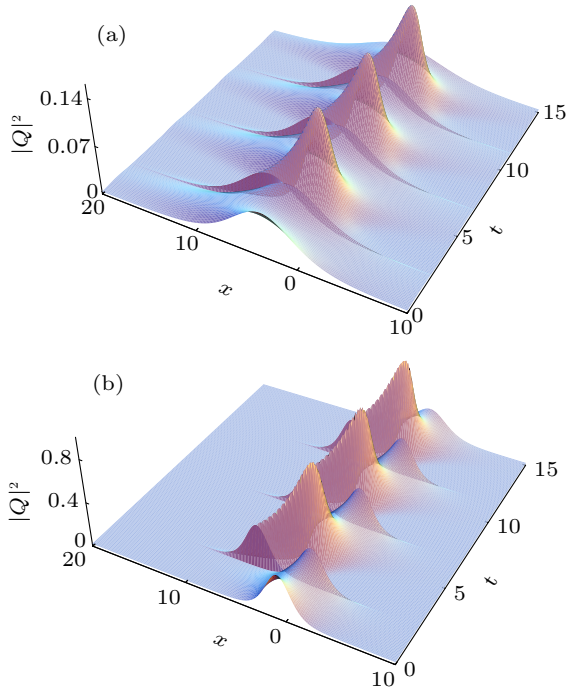


Fig. 6. (color online) The spatiotemporal evolutions of one-soliton densities for (a) $k = 1$ and (b) $k = 0.4$. We set $\gamma_4 = 0.6$ and $\omega_2 = 1.4$. The other parameters are the same as those of Fig. 5.

4. Conclusions and discussion

In summary, we have considered a one-dimensional nonautonomous Gross–Pitaevskii system, where the time-dependent parabolic potential and nonlinearity satisfy the exact integrability scenario. It is well known that a lot of exact one-soliton solutions have been reported for different physical systems, where the soliton amplitudes were consistently described by a standard hyperbolic secant function of spatiotemporal coordinates. There is a very interesting question: does a deformed-soliton solution whose amplitude is deviated from the standard form exist in a nonautonomous NLSE? Utilizing different nonlinearity strengths and corresponding parabolic potentials, we find a set of new exact solutions of the macroscopic wave function and the position of a soliton's center of mass, which describes a nonautonomous deformed one-soliton in an attractive BEC. Furthermore, we study the dynamical behaviors of the deformed-solitons and show some new soliton characteristics of the BEC. On one hand, the deformed soliton has general dynamical characteristics, which include those of the standard one-soliton solutions. On the other hand, defining the deformation factor modulated by the number of condensed atoms and the initial conditions, we reveal some new soliton characteristics, namely, the shape, position, and propagation velocity of the matter-wave deformed soliton can be manipulated by adjusting the deformation factor k, or equivalently, changing the number of condensed atoms and the initial conditions. When $k = 1$, the exact deformed-soliton solution is reduced to the standard nonautonomous one-soliton solution. The results could be generalized to a nonautonomous optical system and other physical systems governed by the NLSE.

It is worth noting that as one of the most attractive topics, a periodical perturbation to an integrable NLSE can lead to a chaotic soliton[44–47] or other chaotic dynamical behaviors.[48–51] When the periodical external potential has a small deviation from the exact integrability scenario, such perturbation exists in our system, which may result in chaotic nonautonomous deformed solitons.

References

[1] Kartashov Y V, Malomed B A and Torner L 2011 *Rev. Mod. Phys.* **83** 247
[2] Strecker K E, Partridge G B, Truscott A G and Hulet R G 2002 *Nature* **417** 150
[3] Dutton Z, Budde M, Slowe C and Hau L V 2001 *Science* **293** 663
[4] Yan J R and Zhou J 2012 *Chin. Phys. B* **21** 060304
[5] Denschlag J, Simsarian J E, Feder D L, Clark C W, Collins L A, Cubizolles J, Deng L, Haglay E W, Helmerson K, Reinhardt W P, Rolston S L, Schnerder B I and Phillips W D 2000 *Science* **287** 97

[6] Eiermann B, Anker Th, Albiez M, Taglieber M, Treutlein P, Marzlin K P and Oberthaler M K 2004 *Phys. Rev. Lett.* **92** 230401
[7] Song C S, Li J and Zong F D 2012 *Chin. Phys. B* **21** 020306
[8] Yao S F, Li Q Y and Li Z D 2011 *Chin. Phys. B* **20** 110307
[9] Li J H and Li Z J 2011 *Chin. Phys. B* **20** 100501
[10] Tang Y, Jin J and Zheng R J 2006 *Chin. Phys. B* **15** 1960
[11] Huang G, Velarde M G and Makarov V A 2001 *Phys. Rev. A* **64** 013617
[12] Burger S, Carr L D, Öhberg P, Sengstock K and Sanpera A 2002 *Phys. Rev. A* **65** 043611
[13] Chong G S, Hai W H and Xie Q T 2003 *Chin. Phys. Lett.* **20** 2098
[14] Shi Y R, Liu C B, Wang G H and Zhou Z G 2012 *Chin. Phys. B* **21** 120307
[15] Zhao L, Yang J, Xie Q Y and Tian M 2012 *Chin. Phys. B* **21** 090304
[16] Poletti D, Alexander T J, Ostrovskaya E A, Li B W and Kivshar Y S 2008 *Phys. Rev. Lett.* **101** 150403
[17] Martin A D, Adams C S and Gardiner S A 2007 *Phys. Rev. Lett.* **98** 020402
[18] Fu L B, Liu J, Zhao H and Wang G F 2005 *Acta Phys. Sin.* **54** 5003 (in Chinese)
[19] Khawaja U Al 2007 *Phys. Rev. E* **75** 066607
[20] Khawaja U Al 2006 *J. Phys. A* **39** 9679
[21] Khawaja U Al 2009 *J. Phys. A* **42** 265206
[22] Liang Z X, Zhang Z D and Liu W M 2005 *Phys. Rev. Lett.* **94** 050402
[23] Degasperis A 2010 *J. Phys. A* **43** 434001
[24] Hai W H, Xie Q T and Rong S G 2011 *Eur. Phys. J. D* **61** 431
[25] Hai W H, Li Y, Xia B L and Luo X B 2005 *Europhys. Lett.* **71** 28
[26] Serkin V N, Hasegawa A and Belyaeva T L 2007 *Phys. Rev. Lett.* **98** 074102
[27] Serkin V N, Hasegawa A and Belyaeva T L 2010 *Phys. Rev. A* **81** 023610
[28] Kumar V R, Radha R and Panigrahi P K 2008 *Phys. Rev. A* **77** 023611
[29] Chen H H and Liu C S 1976 *Phys. Rev. Lett.* **37** 693
[30] Belmonte-Beitia J and Cuevas J 2009 *J. Phys. A* **42** 165201
[31] Chong G and Hai W 2007 *J. Phys. B* **40** 211
[32] Yaroslav V K, Malomed B A and Torner L 2011 *Rev. Mod. Phys.* **83** 247
[33] Kivshar Yuri S and Malomed B A 1989 *Rev. Mod. Phys.* **61** 763
[34] Hermann A H, William S and Wong W S 1996 *Rev. Mod. Phys.* **68** 423
[35] Hasegawa A and Kodama Y 1995 *Solitons in Optical Communication* (Oxford: Clarendon Press)
[36] Li Z J, Hai W, Deng Y and Xie Q 2012 *J. Phys. A* **45** 435003
[37] Hai W H, Lee C H and Chong G S 2004 *Phys. Rev. A* **70** 053621
[38] Hai W H, Xie Q T and Fang J S 2005 *Phys. Rev. A* **72** 012116
[39] Hai W H, Huang S X and Gao K L 2003 *J. Phys. B* **36** 3055
[40] Rietmann M, Carretero-González R and Chacón R 2011 *Phys. Rev. A* **83** 053617
[41] Inouye S, Andrews M R, Stenger J, Miesner H J, Stamper-Kurn D M and Ketterle W 1998 *Nature* **392** 151
[42] He X G, Zhao D, Li L and Luo H G 2009 *Phys. Rev. E* **79** 056610
[43] Hiroki S and Masahito U 2003 *Phys. Rev. Lett.* **90** 040403
[44] Nozaki K and Bekki N 1983 *Phys. Rev. Lett.* **50** 1226
[45] Moon H T and Goldman M V 1984 *Phys. Rev. Lett.* **53** 1821
[46] Zhu Q Q, Hai W H and Rong S G 2009 *Phys. Rev. E* **80** 016203
[47] Zhou Z, Hai W H, Deng Y and Xie Q T 2012 *Chaos Soliton. Fract.* **45** 1423
[48] Lee C H, Hai W H, Shi L, Zhu X W and Gao K L 2001 *Phys. Rev. A* **64** 053604
[49] Hai W H, Lee C H, Chong G S and Shi L 2002 *Phys. Rev. E* **66** 026202
[50] Luo X B, Xia X W and Zhang X F 2010 *Chin. Phys. Lett.* **27** 040302
[51] Wang Z X, Ni Z G, Cong F Z, Liu X S and Chen L 2010 *Chin. Phys. B* **19** 113205